Article:
Vieira Casanova Monteiro, M, Pessu, F, Barker, R orcid.org/0000-0002-5106-6929 et al. (2 more authors) (2019) Analysis of the use of environmentally friendly corrosion inhibitors for mild steel in a carbon dioxide saturated chloride solution via experimental design. Materials and Corrosion, 70 (2). pp. 377-389. ISSN 0947-5117

https://doi.org/10.1002/maco.201810407

Analysis of the use of environmentally-friendly corrosion inhibitors for mild steel in a carbon dioxide saturated chloride solution via experimental design

M. V. C. Monteiro[1], F. Pessu[2], R. Barker[2], J. A. C. Ponciano Gomes[1], A. Neville[2]
[1]LabCorr, Federal University of Rio de Janeiro, Rio de Janeiro/Brazil
[2]Institute of Functional Surfaces, School of Mechanical Engineering, University of Leeds, Leeds, United Kingdom, LS2 9JT

In the oil and gas industry, carbon dioxide (CO_2) gas dissolved in produced fluids can cause both general and localised corrosion of carbon steel pipelines due to the speciation of carbonic acid. To mitigate corrosion, the injection of inhibitors into the production fluid is one of the most commonly used methods. However, recent changes in regulations has resulted in a requirement for the development of new corrosion inhibitors that conform to European regulations. This paper presents a full two-level factorial experimental design approach to study individual effects of environmentally-friendly classed inhibitor components (phosphate ester, imidazoline and quaternary amine derivatives) as combined inhibitors and their interactive effects on carbon steel corrosion processes in CO_2-saturated 3.5 wt.% NaCl brine. Through the application of in situ electrochemical monitoring, post-test interferometry and Scanning Electron Microscopy (SEM) it was possible to determine the influence of each component within the blends and their effect on both general and localised corrosion. Based on 24 hour experiments, the phosphate ester derivative reduced general corrosion rate in all blends; imidazoline derivatives reduced the uniform corrosion rate only when it was at the high level in the blend; and the quaternary amine derivative promoted pitting on the surface.

Keywords: Carbon dioxide corrosion, corrosion inhibitors, environmentally-friendly chemicals, mild steel, phosphate ester, imidazoline, quaternary ammonium salt.

1 Introduction

Internal carbon dioxide (CO_2) corrosion of carbon steel pipelines is a serious and costly problem in the oil and gas industry. [1] Carbon steels are extensively used in this industry, despite being highly susceptible to corrosion under these conditions. [2] This is as a result of their low cost and high level of availability. CO_2, generally present in the fluid produced in the form of dissolved gas, is an influential component in oil field production fluids and its presence permits the formation of carbonic acid, a weak acid which can result in significant levels of corrosion, unless appropriately mitigated. [3-5]

Among the different forms of corrosion control, the application of inhibitors is one of the most common methods, being widely used in oil and gas production systems in order to control internal corrosion of carbon steel structures. [6-7] Such chemicals can be administered through continuous injection, batch treatment, or squeeze treatment. Traditional inhibitors tend to consist predominantly of nitrogen-containing compounds (imidazolines, amines, amides and quaternary ammonium salts) which function by establishing a protective film on the metal surface. [8-10] Several studies have been performed in order to evaluate such compounds' influence in inhibiting carbon steel corrosion in environments containing CO_2. [9-12] However, one limitation of such chemicals is that many of these derivatives do not have a particularly favourable environmental profile and can bioaccumulate, thus imposing restrictions on their use. [13] Some molecules also lack the required level of biodegradability imposed by legislation.

Within the last decade, changes in regulations relating to how the bioaccumulation of surfactants must be characterised has resulted in many previously 'environmentally-friendly' chemicals receiving substitution warnings, meaning they could no longer be classified as 'green inhibitors'. [13] This has resulted in a requirement for the development of new corrosion inhibitors that conform to European regulations. [13] Furthermore, it also casts

doubt over the suitability of any environmentally friendly inhibitors considered in publications prior to 2007, as they may no longer conform to UK regulations. [14-16] As a result, green chemistry and the development of efficient, environmentally friendly corrosion inhibitors has become a significant point of focus within the oil and gas industry. [17]

In terms of chemical classification, a corrosion inhibitor component is classified as environmentally-friendly according to whether it meets the defined limits relating to three criteria: toxicity, bioaccumulation and biodegradation. [18] Considering the increasing environmental concerns, research is focused on producing and testing corrosion inhibitors which conform to the specified limits. [16, 19-23]

The present work highlights the development of an experimental design to study the influence of environmentally-friendly compounds in inhibiting both general and localised corrosion of X65 carbon steel in environments saturated with CO_2. The role of each component is systematically studied across 8 carefully chosen inhibitor blends to elucidate the effect of each component and their synergism with one another when inhibiting both general and localised CO_2 corrosion. This is achieved through a combination of surface analysis, surface profilometry and electrochemical measurements in the form of the linear polarisation resistance technique.

2 Materials and methods

2.1 Materials and sample preparation

10x10x5 mm working electrodes specimens were cut from an API 5L X65 carbon steel bar with a composition (in wt.%) of C: 0.110, Si: 0.140 P: 0.011, S: 0.002, Mo: 0.170, Ni: 0.080, Nb: 0.024, V: 0.090, Mn: 1.360, Cr: 0.120, Cu: 0.07 and Fe: balance. This composition is in accordance to the standard for this particular steel. [24]

Working electrodes were prepared by soldering a wire on the back of each sample and embedding them in non-conducting resin. The exposed surface area per sample was 1 cm^2 and the specimens surfaces were wet ground up to 1200 silicon carbide (SiC) grit paper, rinsed with ethanol and dried with compressed air prior to the start of each experiment.

2.2 Solution preparation

The electrolyte consisted of 1 litre of 3.5% NaCl brine solution. The prepared solution was saturated with CO_2 for a minimum of 4 hours prior to starting each experiment to reduce oxygen concentration, simulating oilfield environments. The pH value after 4 hours was approximately 3.7-3.8 prior to heating. CO_2 was bubbled into the system during the experiments and all tests were conducted at atmospheric pressure. All experiments were conducted at a temperature of 60 ºC in either its unbuffered state (~3.9) or with the addition of sodium bicarbonate to adjust solution pH to 6.6.

2.3 Inhibitors

The tests with inhibitors were performed using three different inhibitory components at two concentrations within the formulated blend: low (L) and high (H); producing eight blends in total. This formulated blend was administered at a total concentration of 10 ppm in all experiment. The low concentration within the blend corresponded to 1.5% and the high concentration within the blend was 15% of the component. Component A is a phosphate ester derivative, component B is an imidazoline derivative and component C is a quaternary amine derivative, which are all environmentally acceptable under CEFAS rules (The Centre for Environment, Fisheries and Aquaculture Science – UK). The addition of each inhibitor blend

to the system was performed after two hours of pre-corrosion. Figure 1 shows the generic structure of the components molecules.

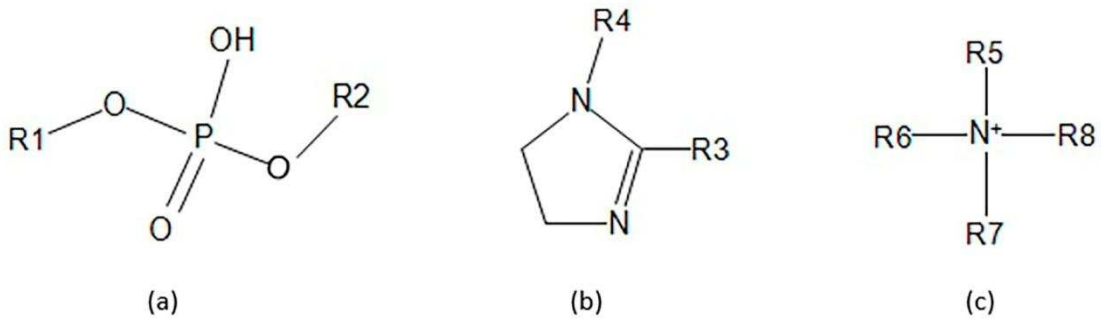

Figure 1. Structures of corrosion inhibitor components used: (a) phosphate ester derivative, (b) imidazoline derivative and (c) quaternary amine derivative. [25, 26]

Besides the three components A, B and C, a sulphur synergist (mercaptoethanol (ME) at 0.5%) and a stabilizer (monoethylene glycol (MEG) at 10%) were also included in the blends. The remaining part of the blend comprised of distilled water. Table 1 shows the blend matrix of the components.

Table 1. Composition of blends for inhibitors evaluation.

Components/ Blends	Phosphate Ester derivative (A)	Imidazoline derivative (B)	Quaternary amine derivative (C)	ME	MEG	Water
1 (LLL)	1.5 %	1.5 %	1.5 %	0.5%	10%	85%
2 (HHH)	15 %	15 %	15 %	0.5%	10%	44.5%
3 (LLH)	1.5 %	1.5 %	15 %	0.5%	10%	71.5%
4 (LHL)	1.5 %	15 %	1.5 %	0.5%	10%	71.5%
5 (HLL)	15 %	1.5 %	1.5 %	0.5%	10%	71.5%
6 (LHH)	1.5 %	15 %	15 %	0.5%	10%	58%
7 (HLH)	15 %	1.5 %	15 %	0.5%	10%	58%
8 (HHL)	15 %	15 %	1.5 %	0.5%	10%	58%

2.4 Experimental and Electrochemical procedure

All experiments were performed in the system shown in Figure 2 and were conducted in static conditions. For all experiments, four 1 cm^2 samples were placed into each cell; two samples for electrochemical measurements and two samples for surface analysis after each experiment. Electrochemical measurements were carried out using an Ivium potentiostat connected to a conventional three-electrode cell, containing an Ag/AgCl reference electrode, platinum counter electrode and one API X65 steel sample at a time as a working electrode.

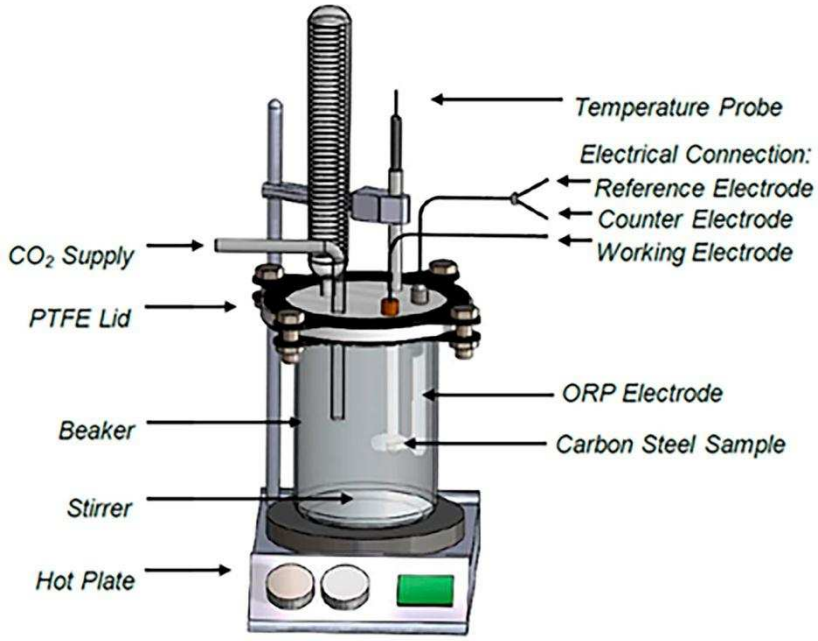

Figure 2. Schematic of test cell for electrochemical measurements to assess the performance of inhibitor blends on carbon steel.

For Linear Polarisation Resistance (LPR) measurements, the one carbon steel sample was polarized ±15 mV about the open circuit potential (OCP) at a scan rate of 0.333 mV s^{-1} to obtain a polarisation resistance, Rp (Ohm cm^2). LPR measurements were undertaken approximately every half hour over the entire test duration of 24 hours. Two samples were then removed from the test solution for surface analysis in the form of interferometry and microscopy. Potentiodynamic Polarisation measurements were obtained from the two

remaining samples by performing anodic and cathodic sweeps individually on each sample. The cathodic sweep was performed first by polarizing from OCP to -500 mV on one sample, before switching to the second sample and polarizing from OCP to +300 mV, both at a scan rate of 0.333 mV s^{-1}.

The resulting polarisation resistance obtained from the LPR measurements was subsequently converted into a corrosion rate through the application of the Stern-Geary relationship (using the measured anodic and cathodic Tafel slopes) and Faraday's Law (Equation 1 to 3).

$$B = \frac{\beta_a \beta_c}{2.303(\beta_a + \beta_c)} \quad (1)$$

$$i_{corr} = \frac{\beta_a \beta_c}{2.303 R_{ct}(\beta_a + \beta_c)} \quad (2)$$

$$CR = \frac{3.27 i_{corr} M_{Fe}}{n\rho} \quad (3)$$

Where βa and βc are the coefficients which characterize the anodic and cathodic Tafel slopes of corrosion process in (V), 3.27 is a conversion factor (mm g (mA cm year)$^{-1}$), i_{corr} is the corrosion current density (mA cm^{-2}), M_{Fe} is the atomic weight of iron = 55.845, n is the number of electrons and ρ the density of iron (g cm^{-3}).

The inhibition efficiency (IE%) was calculated at the end of the experiment and was determined using Equation 4:

$$IE(\%) = \frac{CR_{blank} - CR_{inhib}}{CR_{blank}} x\,100 \quad (4)$$

where CR_{blank} and CR_{inhib} are the final corrosion rates in the absence (blank) and presence of the blends, respectively.

2.5 Characterization of surface tomography and localised attack

Samples selected for surface analysis were removed from the cell after 24 hours, rinsed with distilled water, dried with compressed air and preserved in a desiccator. Each carbon steel specimen was subsequently cleaned with Clarke's solution (20 g antimony trioxide + 50 g

tin(II) chloride and 1000 mL hydrochloric acid) before the analysis in order to remove any potential traces of corrosion product. [27]

Scanning electron microscopy (SEM) analysis was performed using a ZEISS EVO MA 15 and the interferometry measurements were performed using an NPFLEX 3D interferometer. Depth measurements were conducted according to ASTM G46-94. [28] All analysis were done in the central surface area of 9 x 9 mm^2 for each 10 x 10 mm^2 sample face. This consisted of 9 different 3 x 3 mm^2 areas that were stitched together to provide high resolution.

3 Results and Discussion

This section discusses the results obtained in the unbuffered (pH 3.9) and in the pH 6.6 environment at 60 ^oC. From the results in the pH 3.9 system, qualitative and statistical analyses of uniform corrosion data were done, complemented by the morphological analysis of the samples after the tests. Considering results in the unbuffered system, three blends were chosen to be tested in pH 6.6 environment. Qualitative analysis of uniform corrosion data and morphological analysis of tested samples were also performed in these conditions.

3.1 Uniform corrosion in unbuffered system: Inhibitor blend efficiency

Figure 3 shows the results of corrosion rate vs. time when blends 1 to 8 were used at 60 ^oC and pH 3.9, for 24 hours. Each inhibitor blend was administered to the test solution after 2 hours of pre-corrosion. Table 2 indicates the measured Tafel constants and the resulting Stern-Geary coefficients that were implemented when converting the obtained charge-transfer resistances into corrosion rates. The inhibition efficiencies of each blend, based on the final corrosion rates, are presented in Table 3. Figure 4 shows OCP variation with time and the potential difference are presented in Table 4.

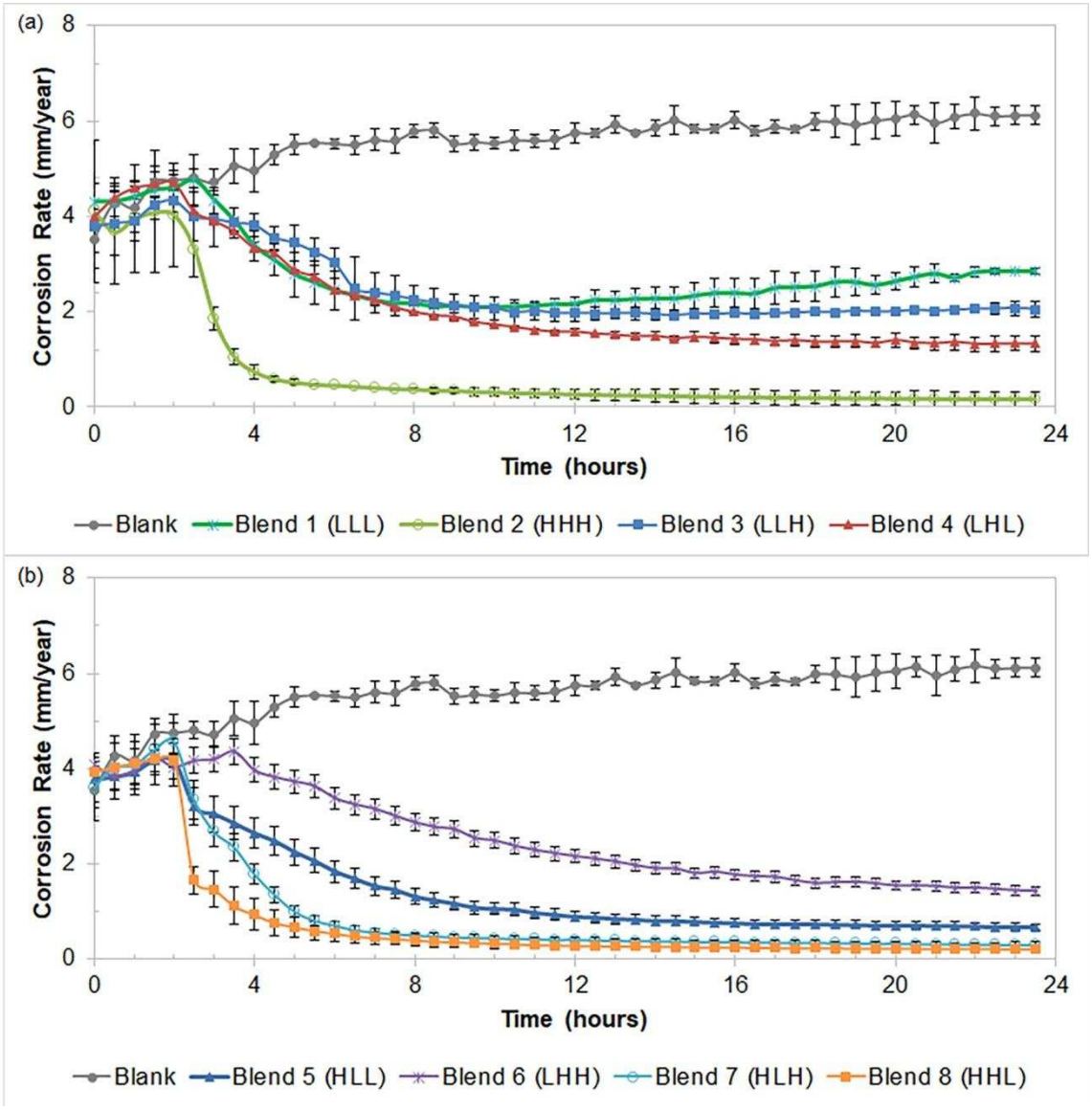

Figure 3. LPR results obtained using X65 carbon steel in 3.5 wt% NaCl solution saturated with CO_2 at 60 °C and pH unbuffered (a) Blank and blends 1-4; (b) Blank and blends 5-8.

Table 2. Tafel constants and Stern-Geary coefficient at different blends at pH 3.9.

	Blank	1 (LLL)	2 (HHH)	3 (LLH)	4 (LHL)	5 (HLL)	6 (LHH)	7 (HLH)	8 (HHL)
β_a (mV/dec)	70	55	60	60	80	70	80	70	60
β_c (mV/dec)	270	250	140	115	125	190	175	190	155
B (mV/dec)	21.31	19.58	18.24	17.12	21.18	22.21	23.84	22.21	18.78

Table 3. Inhibition efficiency of tests using the eight blends.

Blends (ABC)	1 (LLL)	2 (HHH)	3 (LLH)	4 (LHL)	5 (HLL)	6 (LHH)	7 (HLH)	8 (HHL)
General corrosion data: Inhibition efficiency	53%	97 %	66 %	78 %	89 %	76 %	95 %	96 %

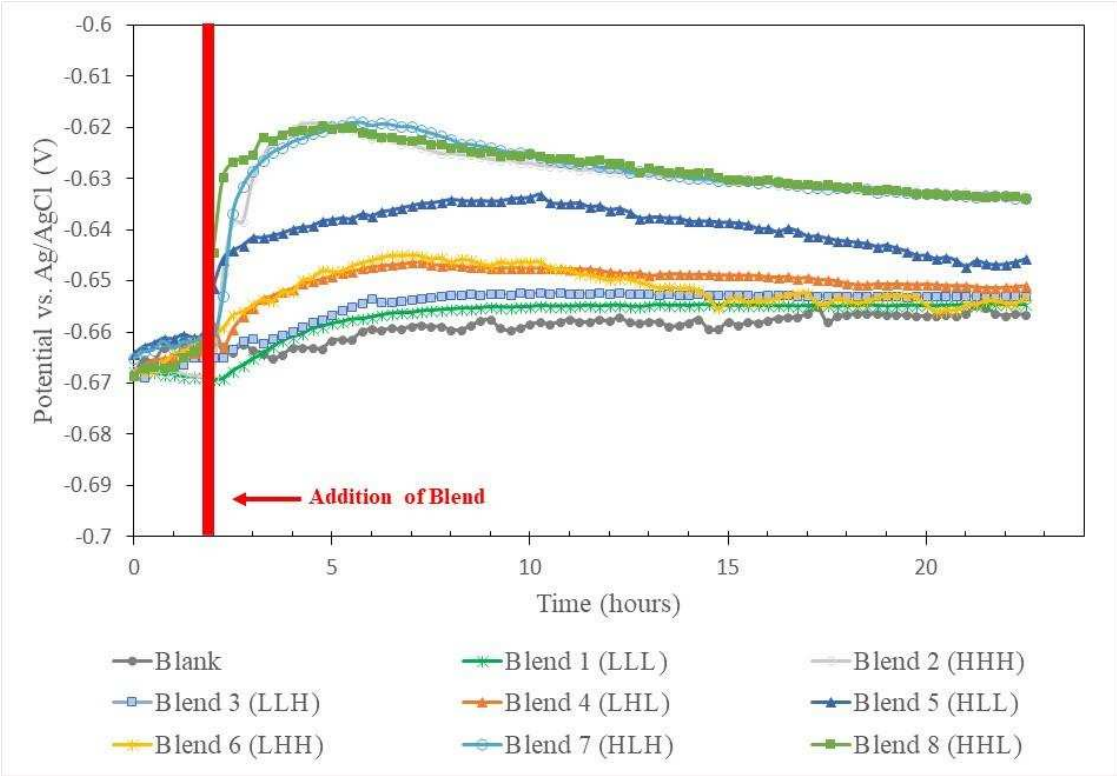

Figure 4. OCP results obtained using X65 carbon steel in 3.5 wt% NaCl solution saturated with CO_2 at 60 °C and pH unbuffered in absence and presence of blends.

Table 4. Potential values of different blends at pH 3.9.

Blend	E_{corr} (V)	ΔE ($E_{corr,blend} - E_{corr,blank}$) (V)
Blank	-0.6566	
Blend 1 (LLL)	-0.6547	0.0019
Blend 2 (HHH)	- 0.6331	0.0235
Blend 3 (LLH)	-0.6529	0.0037
Blend 4 (LHL)	-0.6509	0.0057
Blend 5 (HLL)	-0.6457	0.0109
Blend 6 (LHH)	- 0.6531	0.0035
Blend 7 (HLH)	- 0,6338	0.0228
Blend 8 (HHL)	- 0.6338	0.0228

From Figure 4, it can be seen that the addition of inhibitor shifts the corrosion potential to more positive values, although it is different depending on the inhibitor blend. Blends 2, 7 and 8 presented a major variation than the others. The shift of E_{corr} to more noble value indicate that the blend can effectively inhibit the anodic dissolution of mild steel in tested conditions. The protection mechanism and classification of inhibitor can be determined using the E_{corr} shifts' tendency as follows: when the E_{corr} shifts with and without inhibitor are higher than 85 mV in the anodic or cathodic direction, the compound can be considered an anodic or cathodic inhibitor; while when the potential difference is lower than 85 mV, the inhibitor can be classified as mixed-type inhibitor. [29] Consequently, all blends can be considered mixed-type inhibitors, with the predominant influence on the anodic process. This behavior has been already reported for substances similar to the individual components used in this work. As example, an imidazoline derivative was classified as mixed-type corrosion inhibitor of X65 steel in CO_2-saturated 3 w.t.% NaCl solution, with predominant anodic effect and a phosphate derivative was believed to be a mixed-type inhibitor for carbon steel. [30,31]

3.1.1 Qualitative analysis of A, B and C effects

In Blend 1, all components are at low level and it leads to the lower efficiency in terms of reduction of uniform corrosion as expected. With these components at 1.5% in the blend a reduction of only 53% is achieved. When quaternary amine derivative level is increased, there is an increase in the inhibition efficiency from 53% to 66% (Blend 3 - LLH); increasing imidazoline derivative level, the inhibition efficiency rises from 53% to 78% (Blend 4 - LHL); and when phosphate ester derivative level is increased, the inhibition efficiency displays a strong increment from 53% to 89% (Blend 5 - HLL).

When all the components are at their highest level the corrosion inhibition is higher, achieving 97%. Decreasing phosphate ester derivative (A) level, the inhibition efficiency declines from

97% to 76% (Blend 6 - LHH); decreasing imidazoline derivative (B) level (Blend 7 - HLH) and quaternary amine derivative (C) (Blend 8 - HHL), leads to no significant change in general corrosion inhibition efficiency.

In summary, quaternary amine seems to be the least influential in inhibiting corrosion, since an increase or decrease of C level leads to a lower change in inhibition efficiency. Olivares et al. conclude that the adsorption of oleic imidazoline occurred in a different way to the adsorption of the quaternary amine, or that the adsorption of imidazoline component was stronger than the adsorption of the quaternary amine inhibitor of mild steel in 3% NaCl CO_2-saturated solutions. [32]

Looking at imidazoline derivative (B), a comparison between blends 1 (LLL) and 4 (LHL) shows that an increase only in B level leads to a significant increase in the inhibition efficiency. When blends 3 (LLH) and 6 (LHH) and blends 5 (HLL) and 8 (HHL) are compared separately, it is possible to see a slight increase, from 66% to 76% and from 89% to 96%, respectively. Following the same tendency, when blends 2 (HHH) and 7 (HLH) results are compared, the increase of imidazoline level is less significant. This means that the imidazoline derivative reduces the corrosion rate, but this reduction is more effective when it was at the high level in the blend.

Finally, it is possible to verify that the highest efficiencies are achieved with blends 2 (HHH), 7 (HLH) and 8 (HHL), when phosphate ester derivative (A) level is high. That leads to the conclusion that component A is the most influential on the corrosion inhibition. This behavior where phosphorus-containing molecules are considered to be more effective when compared to nitrogen-containing molecules, as corrosion inhibitors, has been previously reported. [29]

Another observation that contributes to confirm this indication is that when A is at the low level, all inhibition efficiencies are 78% or less. But for components B and C with these at the low level 95% (Blend 7 -HLH) and 96% (Blend 8 - HHL) can be achieved. However it is

important to highlight that in these three systems at least one of the other components (B or C) is also in the high level. Meanwhile, in Blend 5 (HLL) B and C are both at a low level and leading to a drop in the inhibition efficiency. From this, it is possible to verify that component A in high level is not enough to achieve the highest inhibition efficiency and also seems to have a synergism between the components, which raises the efficiencies. Figure 5 summarises the effect of decreasing or increasing components starting from the LLL and HHH blends.

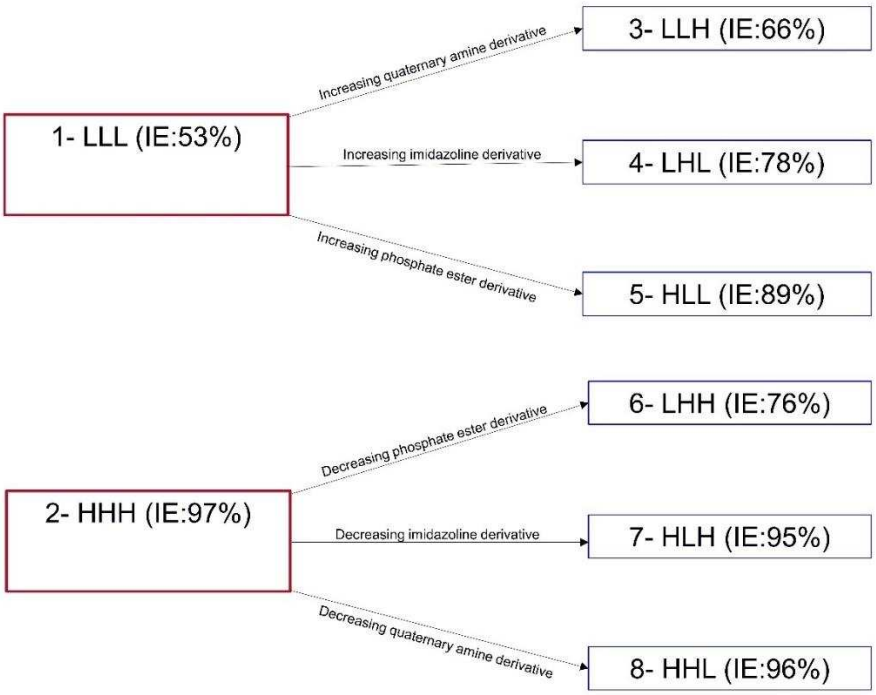

Figure 5. Inhibition efficiency results, based on the final corrosion rates after 24h, obtained changing component levels in a CO_2 saturated system at 60 °C and pH unbuffered.

These observations are from an initial analysis of the results. In a subsequent part of the paper a statistical analysis is done to fully quantify the effects of each inhibitor and more specifically quantify the interactions.

Figure 6 presents the instantaneous efficiency of the blends calculated from LPR results for all blends after 4, 12 and 24 hours of test beginning. The instantaneous efficiency (IE_{inst}) values were calculated using Equation 5:

$$IE_{inst} = \frac{CR_{blank,time} - CR_{inhib,time}}{CR_{blank,time}} \quad (5)$$

where $CR_{blank,time}$ is the corrosion rate value in blank conditions and $CR_{inhib,time}$ is the corrosion rate value in the presence of a blend in a same determinate time. This parameter shows the immersion time dependent inhibition efficiency and, consequently, the blends' capacity of maintain their protective effect, in addition to the speed of corrosion rate drop.

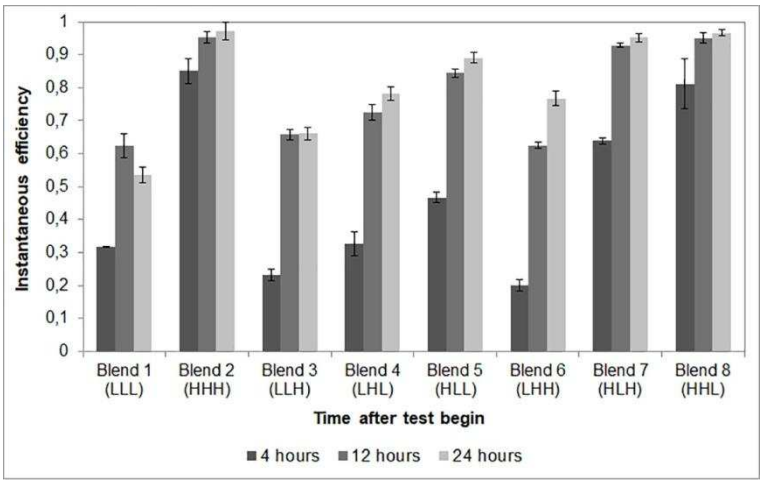

Figure 6. Instantaneous efficiency obtained from LPR results in tests in 60 °C and pH unbuffered, after 4, 12 and 24 hours of test beginning.

With the exception of blends 1 and 3, the instantaneous efficiency increases with time. From the data after 12 and 24 hours, Blend 1 tends to lose their protective effect over time during the experiment. The efficiency of Blend 3 remains similar and blends 2 and 4-8 increase their protective effect on the samples surface. Among the most efficient blends, Blend 2 shows a higher speed of corrosion rate drop, achieving greater efficiencies in a shorter time, followed by blends 8 and 7, respectively.

3.1.2 Statistical analysis: Effects of A, B, C and their interactions

Aiming to calculate the effects of each component and their interactions on general corrosion, the analysis of variance (ANOVA) has been used.

The calculations performed for statistical analysis are provided in Equation 6 to 8: [12]

$$SSq_A = \frac{1}{bc}\sum_{i=1}^{a} y_i^2 - \frac{x^2}{abc} \quad (6)$$

$$SSq_{AB} = \frac{1}{c}\sum_{i=1}^{a}\sum_{j=1}^{b} y_{ij}^2 - \frac{x^2}{abc} - SSq_A - SSq_B \quad (7)$$

$$SSq_{ABC} = \sum_{i=1}^{a}\sum_{j=1}^{b}\sum_{k=1}^{c} y_{ijk}^2 - \frac{x^2}{abc} - SSq_A - SSq_B - SSq_C - SSq_{AB} - SSq_{BC} - SSq_{AC} \quad (8)$$

where SSq are the sum of squares of the respective component or interactions defined in the ANOVA method; a, b and c are the quantity of levels of each component; x are the sum of all corrosion rates and y are the sum of corrosion rate of each condition (levels).

From that, SSq_B, SSq_C, SSq_{BC}, SSq_{AC} can be calculated analogously.

The percentage contribution of each component, CC_X (%) and their interactions CC_{XY} (%), is calculated using Equation 9 to 15: [12]

$$CC_A(\%) = \frac{SSq_A}{SSq_A + SSq_B + SSq_C + SSq_{AB} + SSq_{AC} + SSq_{BC} + SSq_{ABC}} X\ 100 \quad (9)$$

$$CC_B(\%) = \frac{SSq_B}{SSq_A + SSq_B + SSq_C + SSq_{AB} + SSq_{AC} + SSq_{BC} + SSq_{ABC}} X\ 100 \quad (10)$$

$$CC_C(\%) = \frac{SSq_C}{SSq_A + SSq_B + SSq_C + SSq_{AB} + SSq_{AC} + SSq_{BC} + SSq_{ABC}} X\ 100 \quad (11)$$

$$CC_{AB}(\%) = \frac{SSq_{AB}}{SSq_A + SSq_B + SSq_C + SSq_{AB} + SSq_{AC} + SSq_{BC} + SSq_{ABC}} X\ 100 \quad (12)$$

$$CC_{AC}(\%) = \frac{SSq_{AC}}{SSq_A + SSq_B + SSq_C + SSq_{AB} + SSq_{AC} + SSq_{BC} + SSq_{ABC}} X\ 100 \quad (13)$$

$$CC_{BC}(\%) = \frac{SSq_{BC}}{SSq_A + SSq_B + SSq_C + SSq_{AB} + SSq_{AC} + SSq_{BC} + SSq_{ABC}} X\ 100 \quad (14)$$

$$CC_{ABC}(\%) = \frac{SSq_{ABC}}{SSq_A + SSq_B + SSq_C + SSq_{AB} + SSq_{AC} + SSq_{BC} + SSq_{ABC}} X\ 100 \quad (15)$$

The calculations were computed with the use of Design-Expert® Software Version 10. Table 5 shows the contribution of each component and their interactions on the general corrosion calculated by the analysis of variance approach, from the final values of general corrosion rate (shown previously in Figure 3).Component A mostly contributes to general corrosion inhibition, followed by component B. Component C and the interactions AB, AC. BC and ABC presented a contribution percentage less than 5% each, demonstrating a minor contribution to the corrosion inhibition.

Table 5. Contributions of each component and their interaction to inhibition of general corrosion.

Interactions	A	B	C	AB	AC	BC	ABC
Contribution (%)	75.5	14.3	2.3	4.7	0.1	2.7	0.5

Considering the identification of the components that have significant effect (Table 5), an empirical relationship was developed for general corrosion inhibition. From this equation it is possible to calculate an approximated corrosion rate for this system for a given level of A and B. The empirical relationship is based only on A and B values because, as Table 5 shows, the contributions of C, AB, AC, BC and ABC were less than 5%. Here, the levels should be specified in percentage.

$$CR = 2.51711 - 0.11747*A - 0.051062*B \quad (13)$$

For instance, when A level is 15% and B and C level are 1.5%, the corrosion rate calculated by the equation is equal to 0.7 mm $year^{-1}$. A 2D-countour plot of this empirical relationship is presented in Figure 7.

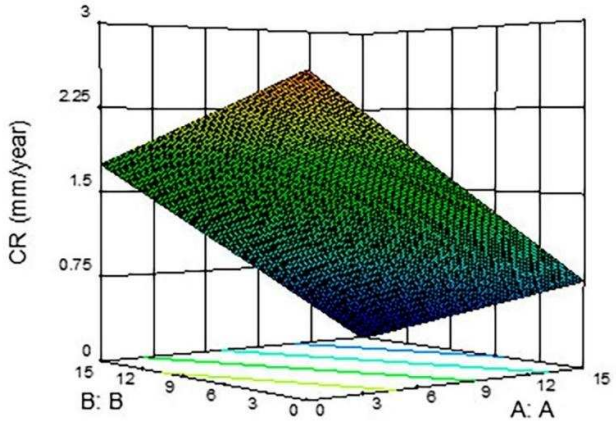

Figure 7. 2D-Contour plot of empirical relationship of general corrosion inhibition.

It is possible to conclude that the statistical analysis had corroborated the qualitative results, showing that compound A has great influence on inhibition, followed by compound B. The empirical equation shows the influence of the compounds and it is important for optimizing blends' formulation. Table 6 shows the eight experimental corrosion rates and predicted results based on the empirical relationship.

Table 6. Final experimental corrosion rates and predicted results of all eight blends.

Blend	Final experimental corrosion rate (mm/year)	Predicted corrosion rate result (mm/year)
1 (LLL)	2.9	2.3
2 (HHH)	0.2	0
3 (LLH)	2.1	2.3
4 (LHL)	1.3	1.6
5 (HLL)	0.7	0.7
6 (LHH)	1.4	1.6
7 (HLH)	0.3	0.7
8 (HHL)	0.2	0

3.2 Surface morphological analysis in unbuffered system

The statistical analysis of corrosion rates has shown the important components for inhibition. Detailed surface analysis was conducted after 24 h of testing to enable the differences in surface morphology to be linked to these results. Figure 8 shows images obtained from the scanning electron microscope at two different magnifications. It was possible to verify the corrosion of the sample with the dissolution of the ferrite. No significant formation of corrosion products were formed under these conditions.

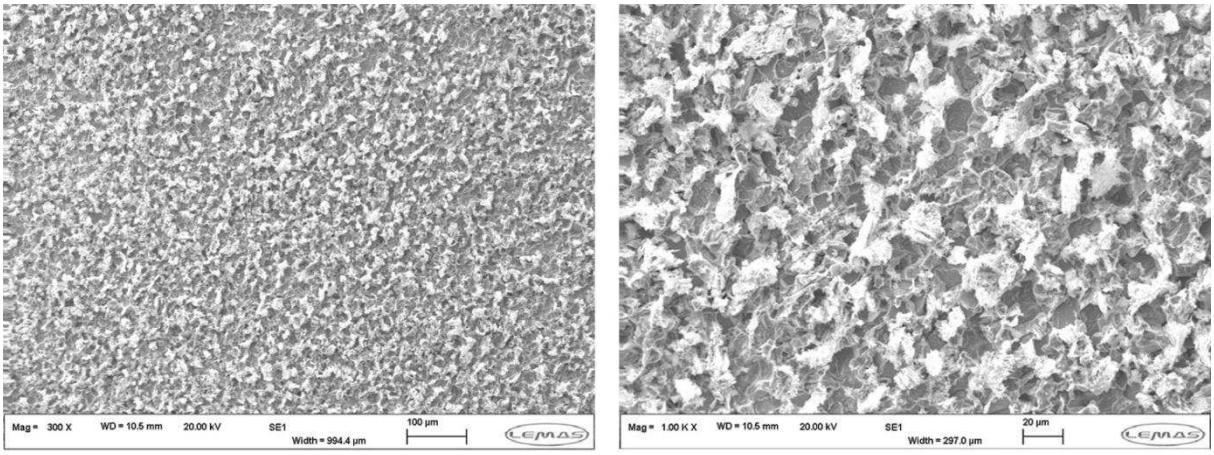

Figure 8. SEM of X65 steel surface after 24 hour tests at 60 °C and pH unbuffered (a) 300x and (b) 1000x.

Figure 9 shows interferometry analysis performed under the same conditions. It is possible to verify the irregularity of the baseline profilometer showing that there was severe corrosion of the sample corroborating with electrochemical results.

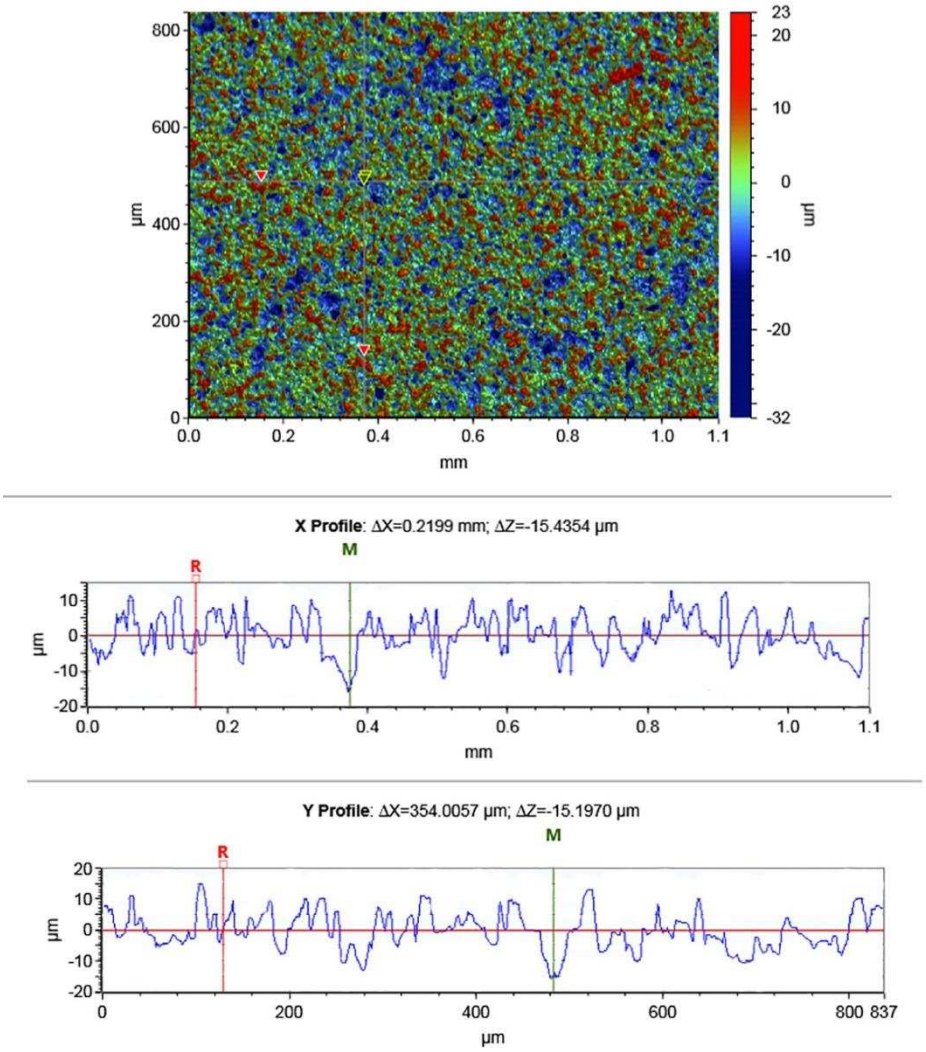

Figure 9. Interferometry after tests at 60 °C and pH unbuffered.

SEM and interferometry analysis were performed in samples tested using all blends. From the analysis it is possible to verify that pits did not occur on samples when blends 1 (LLL), 2 (HHH) and 8 (HHL) were used. In samples from tests using blends 4 (LHL) and 5 (HLL), a localised attack could be observed. It is also possible to verify that pits had occurred when blends 3 (LLH) and 7 (HLH) were used and pits and localised corrosion occurred when Blend 6 (LHH) was used. Therefore, only the most relevant 3D images of interferometry, where identified pits existed are shown in this paper (Figure 10). The tests were 24 hours in duration in this work and it is apparent that for a more detailed study of pitting longer tests will be required.

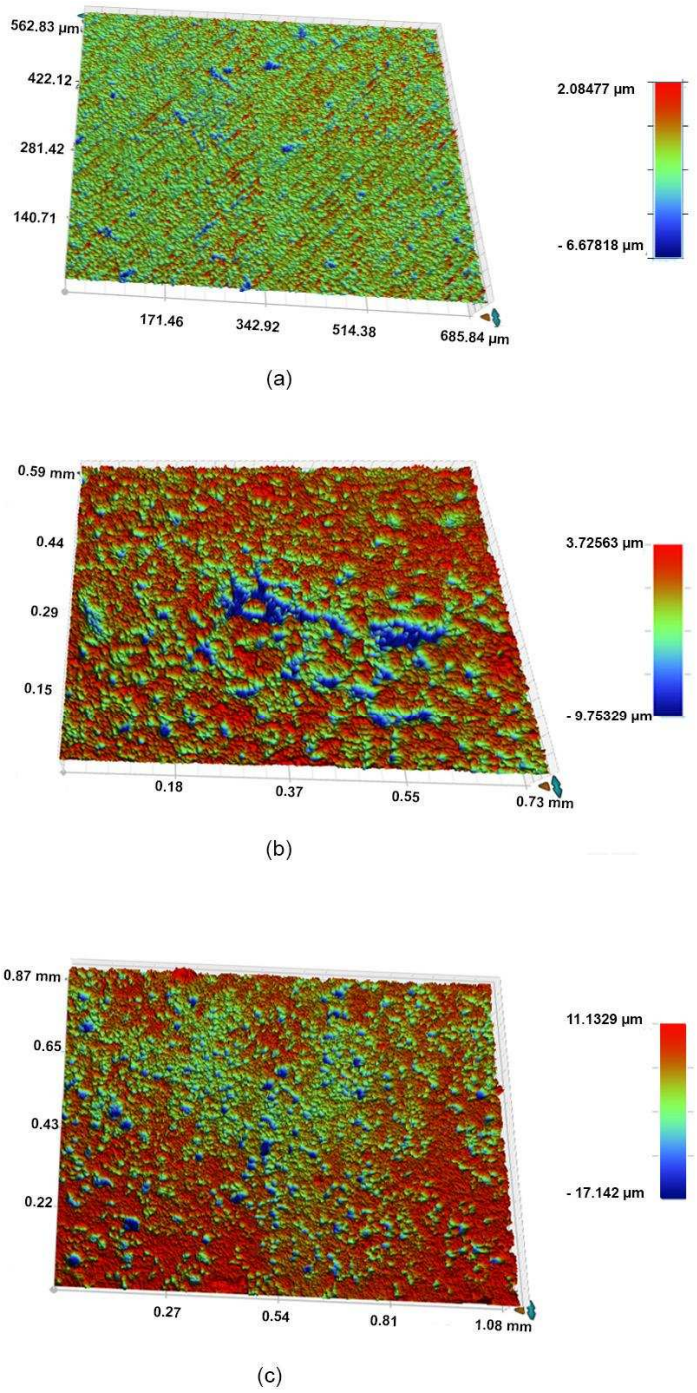

Figure 10. Interferometry results obtained using carbon steel in NaCl solution saturated with CO_2 at 60 °C and pH unbuffered using blends (a) 3, (b) 6 and (c) 7.

The maximum pit and the average penetration depth in the three blends that present pits on the surface are shown in Figure 11. Blend 6 presented higher maximum pit depth, because more localised corrosion occurred in tests using this blend.

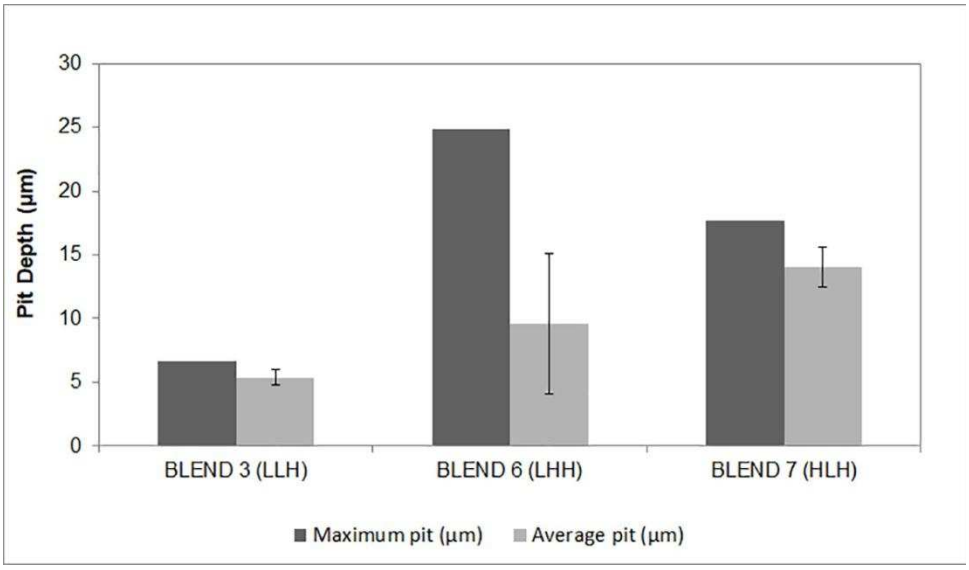

Figure 11. Interferometry results obtained using carbon steel in NaCl solution saturated with CO_2 at 60 °C and pH unbuffered using blends 3, 6 and 7.

3.3 Comparison between uniform and localised corrosion blends efficiencies

Table 7 summarises the uniform corrosion inhibition efficiency and morphological analysis of each blend in pH the 3.9 environment. Considering these results, phosphate ester derivative promotes the reduction of corrosion rate in all blends from the perspective of general corrosion. The imidazoline derivatives reduced the general corrosion rate, especially when it was at the high level in the blend. And the quaternary amine derivative seems to promoted more pits on the surface, probably due to a non-uniform surface protection of the sample surface. Moreover, blends 2 and 8 had presented the most satisfactory results in terms of uniform and localised corrosion in tested conditions.

Table 7. Comparison of uniform and morphological results obtained using each blends in pH 3.9 environment.

Blend	Uniform corrosion data	Morphological analysis
Blend 1 (LLL)	Inhibition efficiency: 53%	no pits
Blend 2 (HHH)	Inhibition efficiency: 97%	no pits
Blend 3 (LLH)	Inhibition efficiency: 66%	pits
Blend 4 (LHL)	Inhibition efficiency: 78%	localised attack
Blend 5 (HLL)	Inhibition efficiency: 89%	localised attack
Blend 6 (LHH)	Inhibition efficiency: 76%	pitting and localised corrosion
Blend 7 (HLH)	Inhibition efficiency: 95%	severe pitting
Blend 8 (HHL)	Inhibition efficiency: 96%	no pits

3.4 Uniform corrosion in pH 6.6 environment

Considering the results at 60 °C and pH unbuffered, tests were also performed using blends 1 (low efficiency), 2 (high efficiency) and 6 (medium efficiency) at 60 °C and a higher pH of 6.6, in order to enhance the study of the interactions between blend components.

Table 8 indicates the measured Tafel constants and the resulting Stern-Geary coefficient in these conditions and Figure 12 shows the results of corrosion rate when blends 1, 2 and 6 were used in tests at 60 °C and pH 6.6, for 24 hours. A concentration of 10 ppm of blend was added in the system.

Table 8. Tafel constants Stern-Geary coefficient at different conditions at pH 6.6.

	Blank	1 (LLL)	2 (HHH)	6 (LHH)
β_a (mV/dec)	90	55	65	85
β_c (mV/dec)	120	100	180	100
B (mV/dec)	22.33	15.41	20.74	19.95

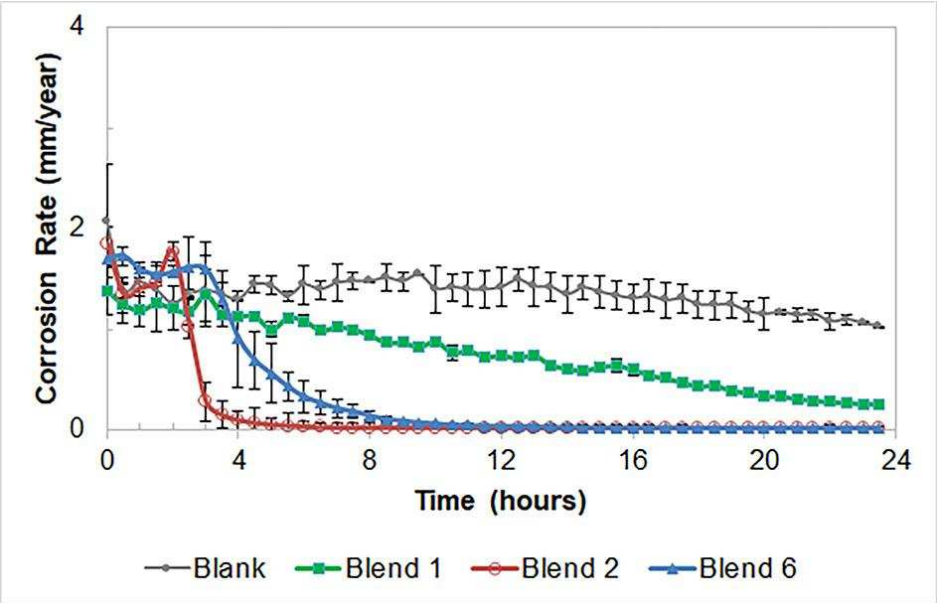

Figure 12. LPR results obtained using carbon steel in NaCl solution saturated with CO_2 at 60 °C and pH 6.6 with and without the addition of 10 ppm of blends 1 (LLL), 2 (HHH) and 6 (LHH), after 24 hours.

Higher pH values cause a lower solubility of iron carbonate ($FeCO_3$), increasing the potential for precipitation. [33] The $FeCO_3$ film formation affects the corrosion rate when the pH value is increased, as can be observed by comparing Figure 3 with Figure 12 under both blank conditions. Blend 2 (HHH) presented the highest efficiency in the shortest time. Moreover, Blend 6 (LHH) presented similar efficiency as Blend 2 after about 11 hours. The inhibition efficiency values are shown in Table 9.

Table 9. Inhibition efficiency of tests using the blends at pH 6.6.

Blends (ABC)	1 (LLL)	2 (HHH)	6 (LHH)
General corrosion data: Inhibition efficiency	76%	99 %	99 %

Figure 13 shows OCP variation with time at pH 6.6 and the potential difference are presented in Table 10. From Figure 13, it can be seen that the addition of inhibitor shifts the corrosion potential to more positive values, as has been obtained in pH 3.9 environment tests. Consequently, all blends can be considered mixed-type inhibitors, with the predominant influence on the anodic process. This behavior has been observed in pH 3.9 environment

experiments and has been already reported. [30,31] As before noticed, Blend 2 presented a major variation than the others and the shift of E_{corr} to more noble values, indicating that this blend is more effective in inhibit the anodic dissolution of mild steel in tested conditions.

Table 10. Potential values of different blends at pH 6.6.

Blend	E_{corr}	ΔE ($E_{corr,\ blend} - E_{corr,\ blank}$) (V)
Blank	-0.71845	
Blend 1 (LLL)	-0.70139	0.01706
Blend 2 (HHH)	-0.65130	0.06715
Blend 6 (LHH)	-0.66448	0.05397

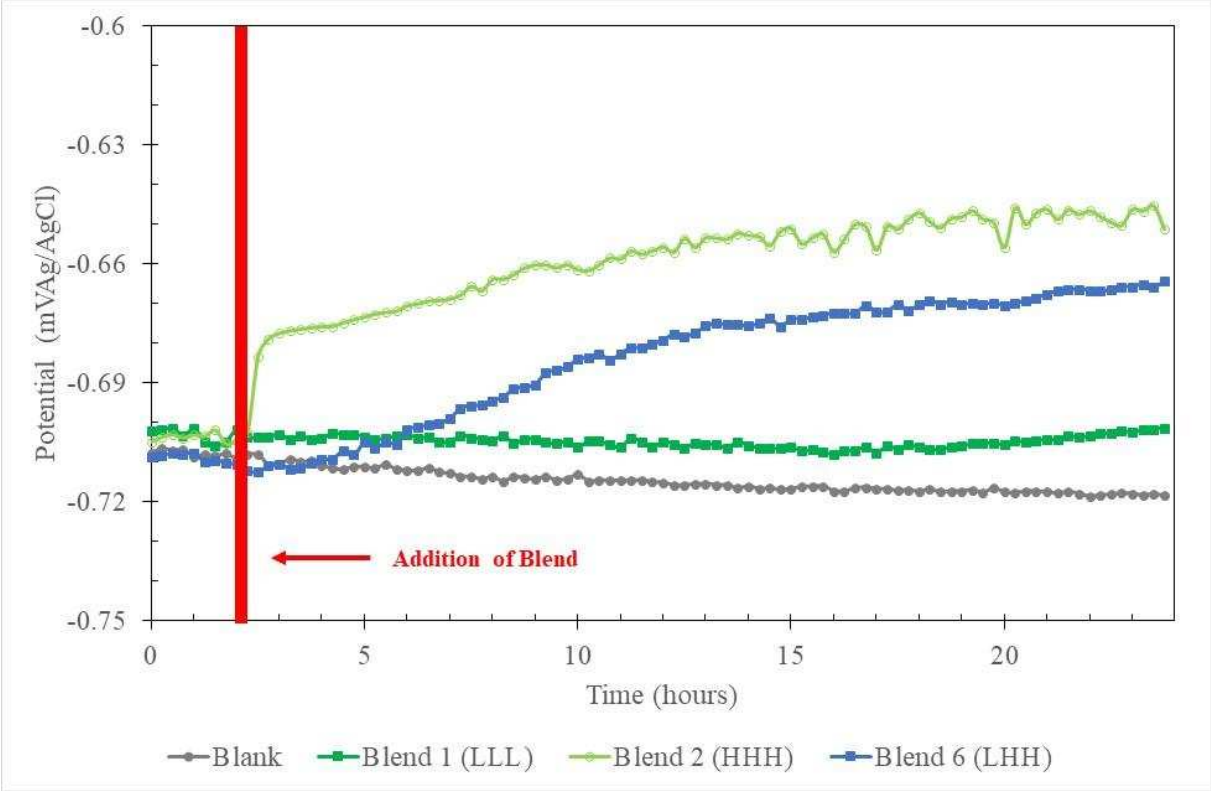

Figure 13. OCP results obtained using X65 carbon steel in 3.5 wt% NaCl solution saturated with CO_2 at 60 °C and pH 6.6 in absence and presence of blends.

3.5 Surface morphological analysis in the pH 6.6 environment

Figure 14 shows SEM analysis of a sample after a blank test (after removal of corrosion products) and Figure 15 shows the SEM and interferometry analysis for the three blends. The interferometry results showed that there are pits on the surface only when Blend 1 was used. Comparing results at pH 6.6, lower levels of the components cause pitting on the surface. When the level of imidazoline derivative and quaternary amine derivative are increased no localised corrosion can be observed.

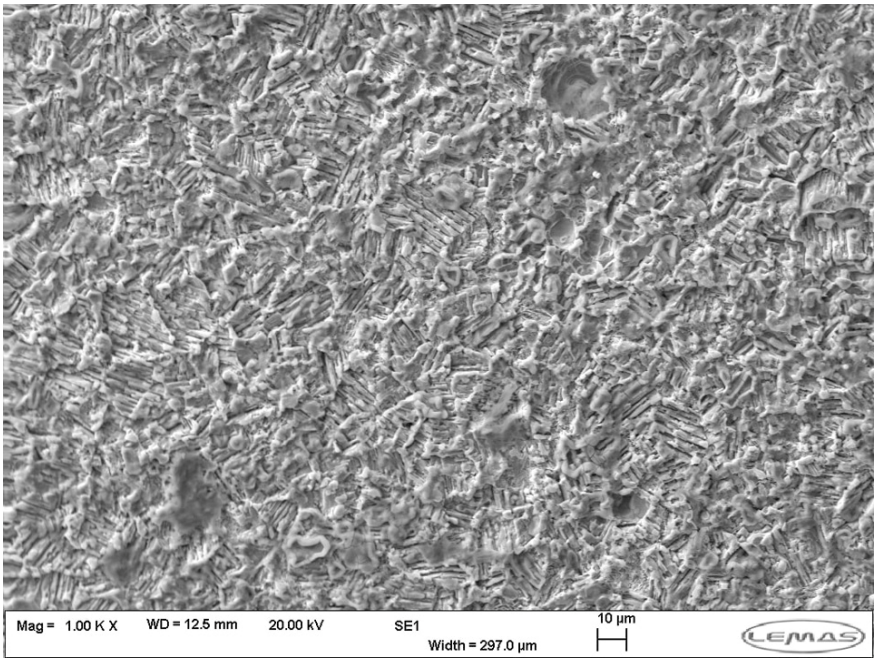

Figure 14. SEM analysis after test at 60 ºC and pH 6.6 in blank conditions, after 24 hours.

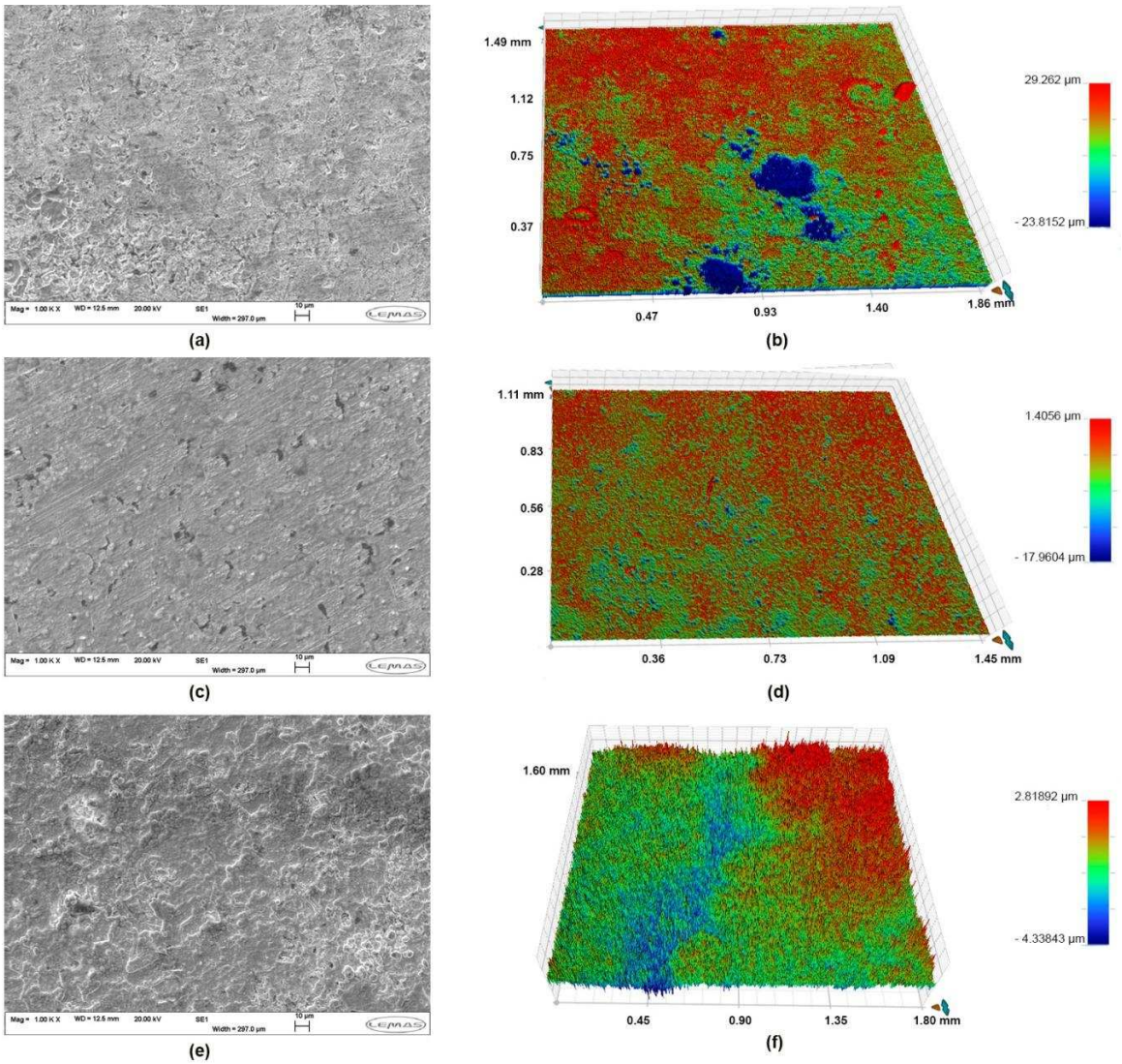

Figure 15. SEM and Interferometry results after tests at 60 ºC and pH 6.6 using blends 1 (a-b), 2 (c-d) and 6 (e-f).

3.6 Comparison of results obtained using blends 1, 2 and 6 in pH 3.9 and pH 6.6 environments

In the beginning of the tests, before the addition of the blends (pre-corrosion time), it is possible to verify from Figure 3 and 11 that the corrosion rate value is already lower in pH 6.6 than in pH 3.9 environment. It was known that pH value has a substantial influence on the corrosion rate. In unbuffered systems the reaction of reduction of H^+ ions is relevant and it has a direct effect on the corrosion rate.

The sample surface changes depending on the pH value. At pH 3.9, iron carbide (Fe_3C) is commonly observed on the carbon steel surface after CO_2 corrosion. A higher pH value results in $FeCO_3$ film formation, due to lower $FeCO_3$ solubility. At pH 6.6 a formation of protective scales and a decrease of the corrosion rate with time can occur. [33-34]

It is possible to observe in Figure 12 that film formation cannot be seen in LPR measurements before about 7 hours (when corrosion rate in blank conditions starts to decrease). Such behaviour is consistent with observations by other authors, where the nucleation of $FeCO_3$ crystals on the steel surface after 7 hours of the test beginning has been shown. [34]

Considering the addition of the inhibitors and the results in the two different pH environments it is possible to observe that all blends resulted in more efficient inhibition at pH 6.6 than at pH 3.9. Blend 2 is efficient in inhibiting general and localised corrosion in tested conditions, both at pH 3.9 and 6.6. When Blend 1 was used, there were no pits on the surface at pH 3.9, but it was possible to observe pits at pH 6.6. This is likely to be because of the non-uniform protection of surface films. Results using Blend 6 were improved both in inhibition efficiency and localised corrosion, at pH 6.6. Therefore, it is possible to conclude that the efficiency of an inhibitor at a pH value does not guarantee the same efficiency at different pH values. Table 11 summarises this information.

Table 11. Comparison of results obtained using blends 1, 2 and 6 in pH 3.9 and pH 6.6.

Blend	pH 3.9	pH 6.6
Blend 1 (LLL)	Inhibition efficiency: 53% no pits	Inhibition efficiency: 76% pits on the surface
Blend 2 (HHH)	Inhibition efficiency: 97% no pits	Inhibition efficiency: 99% no pits
Blend 6 (LHH)	Inhibition efficiency: 76% pitting and localised corrosion	Inhibition efficiency: 99% no pits

4 Conclusions

The following main conclusions were obtened in the present work:

1. A mixture containing environmentally-friendly components, phosphate ester derivative, imidazoline derivative and quaternary amine derivative, can be used as an efficient corrosion inhibitor of X65 carbon steel in a CO_2 environment after the optimization done by the experimental design methodology applied. All blends can be classified as mixed-type inhibitor in tested conditions.

2. Blend 2 had presented the most satisfactory inhibition efficiencies in terms of uniform and localised corrosion in both pH environments, since it had promoted the lowest corrosion rate in the electrochemical measurements and had not presented localized corrosion in SEM and interferometry analysis.

3. The phosphate ester derivative is the most influential component on the corrosion inhibition, what can be conclude by the highest efficiencies that were achieved with blends 2 (HHH), 7 (HLH) and 8 (HHL) at pH 3.9, where this component was at a high level.

4. Phosphate ester derivative at a high level is not enough to achieve the highest inhibition efficiency and also seems to have a synergism between the components, which raises the efficiencies values. In Blend 5 (HLL), imidazoline derivative and quaternary amine derivative are both at a low level and leading to a drop in the inhibition efficiency.

5. An empirical relationship for general corrosion inhibition was developed from statistical analysis and that can be used for optimising blends' formulation.

6. From morphological analysis in blends 3 (LLH), 6 (LHH) and 7 (HLH), where quaternary amine derivative was at a high level, it was possible to verify that this component seems to promoted more pits on the surface. It had probably occurred due to a non-uniform surface protection of the sample surface.

Acknowledgements

The authors would like to thanks CNPq, ANP and Shell for the support.

5 References

[1] T. C. Bayram, N. Orbey, R. Y. Adhikari, M. Tuominen, Prog. Org. Coat. **2015**, 88, 54.

[2] S. D. Zhu, A. Q. Fu, J. Miao, Z. F. Yin, G. S. Zhou, J. F. Wei, Corros. Sci. **2011**, 53, 3156.

[3] Q. Y. Liu, L. J. Mao, S. W. Zhou, Corros. Sci. **2014**, 84, 165.

[4] R. Barker, X. Hu, A. Neville, S. Cushnaghan, Corrosion. **2013**, 69, 193.

[5] A. Singh, Y. Lin, E. E. Ebenso, W. Liu, J. Pan, B. Huang, J. Ind. Eng. Chem. **2015**, 24, 219.

[6] P. B. Raja, M. G. Sethuraman, Mater. Lett. **2008**, 62, 2977.

[7] L. M. Rivera-Grau, M. Casales, I. Regla, D. M. Ortega-Toledo, J.G. Gonzalez-Rodriguez, L. Martinez Gomez, Int. J. Electrochem. Sci. **2012**, 7, 13044.

[8] X. Zhang, F. Wang, Y. He, Y. Du, Corros. Sci. **2001**, 43, 1417.

[9] L.D. Paolinelli, T. Pérez, S. N. Simison, Corros. Sci. **2008**, 50, 2456.

[10] M. Heydari, M. Javidi, Corros. Sci. **2012**, 61, 148.

[11] A. Singh, Y. Lin, K. R. Ansari, M. A. Quraishi, E. E. Ebenso, S. Chen, W. Liu, Appl. Surf. Sci. **2015**, 359, 331.

[12] M. Ciolkowski, A. Neville, presented at Corrosion 2004, Paper nº 3960, NACE International, New Orleans **2014**.

[13] A. Jenkins, presented at Corrosion 2011, Paper nº 11272, NACE International, Houston **2011**.

[14] M. H. Hussin, M. J., Kassim, Mater. Chem. Phys. **2011**, 125, 461.

[15] J. C. Rocha, J. A. C. P. Gomes, E. D'Elia, Corros. Sci. **2010**, 52, 2341.

[16] N. D. Nam, Q. V. Bui, M. Mathesh, M. Y. J. Tan, M. Forsyth, Corros. Sci. **2013**, 76, 257.

[17] X. Sun, L. Yu, Mater. Corros. **2018**, 1.

[18] A. Martinod, A. Neville, M. Euvrad, K. Sorbie, Chem. Eng. Sci. **2009**, 64, 2413.

[19] E. Chaieb, A. Bouyanzer, B. Hammouti, M. Berrabah, Acta Phys. Chim. Sin. **2009**, 25, 1254.

[20] H. M. Abd El-Lateef, L. I. Aliyeva, V. M. Abbasov, T. I. Ismayilov, Adv. Appl. Sci. Res. **2012**, 3, 1185.

[21] C. B. Verma, M. A. Quraishi, A. Singh, J. Taiwan Inst. Chem. Eng. **2015**, 49, 229.

[22] M. N. El-Haddad, Carbohydr Polym, **2014**, 112, 595.

[23] B. Zhang, C. He, C. Wang, P. Sun, F. Li, Y. Lin, Corros. Sci. **2015**, 94, 6.

[24] API SPECIFICATION 5L: API Specification for Line Pipe, American Petroleum Institute, 44º ed. **2007**.

[25] B. D. B. Tiu, R.C. Advincula, React. Funct. Polym. **2015**, 95, 25.

[26] J.E. Wong, N. Park, presented at Corrosion 2009, Paper n° 09569, NACE International, **2009**.

[27] ASTM G1-03, ASTM International, Conshohocken, **2011**.

[28] ASTM G46-94, ASTM International, Conshohocken, **2013**.

[29] B. D. B. Tiu, R. C. Advincula, React. Funct. Polym. **2015**, 95, 25.

[30] I. Jevremović, M. Singer, S. Nešić, V. Mišković-Stanković, Mater. Corros. **2016**, 67, 756.

[31] M.A. Hegazy, A.S. El-Tabei, A.H. Bedair, M.A. Sadeq, Corros. Sci. **2012**, 54, 219.

[32] G. Zavala Olivares, M. J. Hernandez Gayosso, J. L. Mora Mendoza, Mater. Corros. **2007**, 58, 427.

[33] S. Nešić, Corros. Sci. **2007**, 49, 4308.

[34] F. Pessu, R. Barker, A. Neville, presented at Corrosion 2015, Paper n° 5584, NACE International, Dallas **2015**.

Graphical Abstract

Eight blends prepared based on a full two-level factorial experimental desing, using three eco-friendly components, have been evaluated as corrosion inhibitors for mild steel at 60 °C in a CO_2-saturated brine. The results showed that is possible to determine each component influence within the blends and optimize formulation in determinated experimental conditions, from statistical analysis.